Science Advances
AAAS

advances.sciencemag.org/cgi/content/full/7/12/eabf7412/DC1

Supplementary Materials for

Temporal mechanisms of myogenic specification in human induced pluripotent stem cells

P. Nayak, A. Colas, M. Mercola, S. Varghese*, S. Subramaniam*

*Corresponding author. Email: shankar@ucsd.edu (S.S.); shyni.varghese@duke.edu (S.V.)

Published 17 March 2021, *Sci. Adv.* **7**, eabf7412 (2021)
DOI: 10.1126/sciadv.abf7412

This PDF file includes:

Supplementary Materials

Figure S1

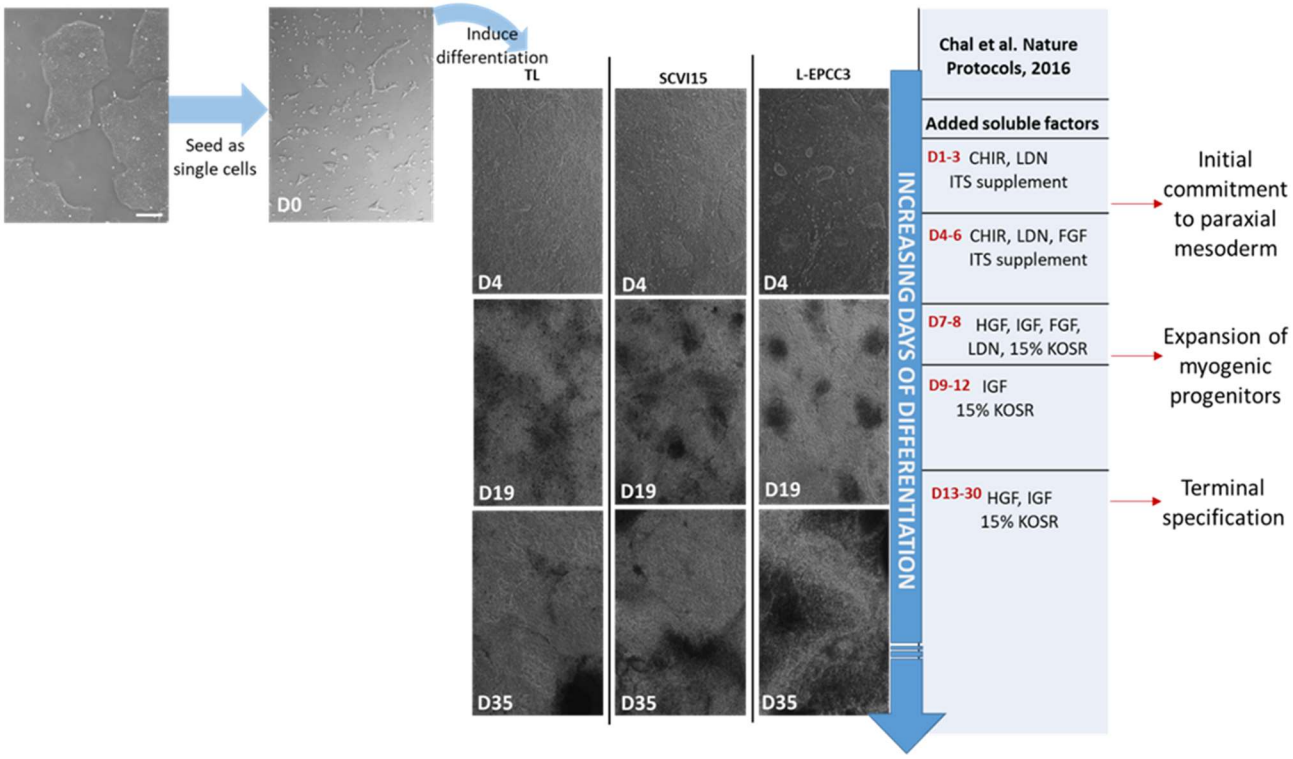

Fig. S1 Myogenic induction protocol with corresponding cell-line dependent gross morphological changes

Briefly, this protocol achieves initial mesoderm induction via Wnt activation through GSK3β inhibition by CHIR, as well as modulation of Tgfβ family signaling by LDN18098. The mesodermal cell population is selectively expanded by the addition of FGF2 and HGF followed by induction of terminal specification of the myogenic progenitors with IGF and HGF supplementation. Comparison of gross morphological changes shows similar trends, as the cell lines reach confluence by day three and then form areas of higher cell density, which are more prominent in the LEPCC3 line

Figure S2

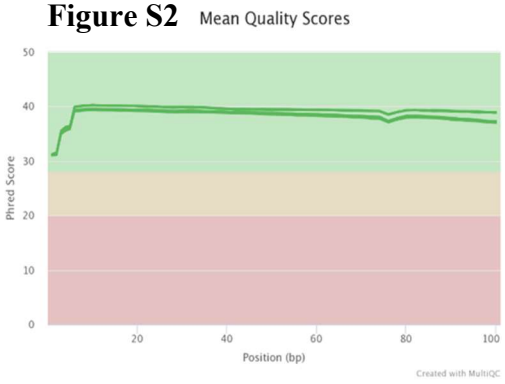

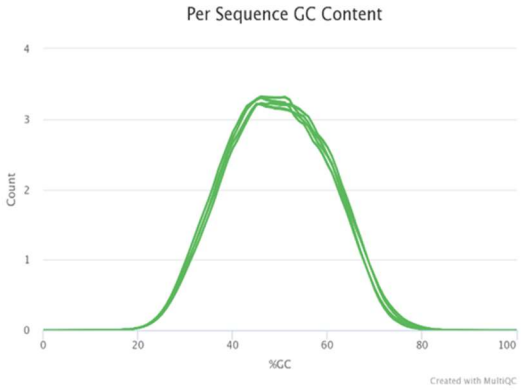

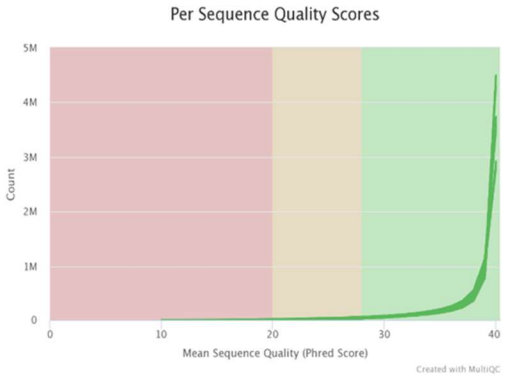

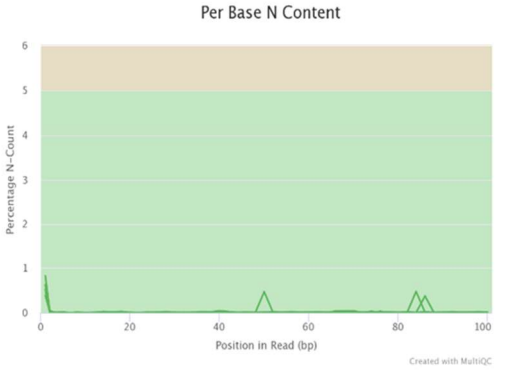

Representative proportion of reads aligned

Sample Name	% Aligned	M aligned
LEPCC3_D0_1	87.90%	26.2
LEPCC3_D0_2	86.20%	27.4
LEPCC3_D3_1	88.70%	22.6
LEPCC3_D3_2	90.20%	27.3
LEPCC3_D6_1	87.30%	31.7
LEPCC3_D6_2	88.30%	34.5
LEPCC3_D8_1	86.80%	29.5
LEPCC3_D8_2	85.80%	33.2
LEPCC3_D12_1	87.60%	30.2
LEPCC3_D12_2	88.30%	25.8
LEPCC3_D16_1	86.00%	30.1
LEPCC3_D16_2	86.30%	25
LEPCC3_D19_1	84.70%	28.3
LEPCC3_D19_2	86.70%	28.4
LEPCC3_D25_1	86.70%	26.2
LEPCC3_D25_2	85.80%	26.5
LEPCC3_D30_1	83.90%	28.3
LEPCC3_D30_2	85.90%	32.6

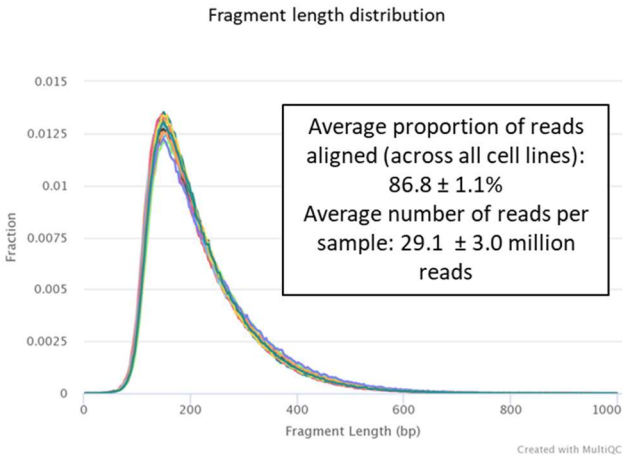

Fig. S2 High quality raw reads with good alignment to GRCh38 transcriptome

Initial raw read quality assessment with FastQC (Babraham Bioinformatics) showed overall high quality reads, with representative images shown above. Alignment to the GRCh38 human transcriptome, including coding and noncoding transcripts resulted in about 87% of reads successfully aligned across all samples.

Figure S3

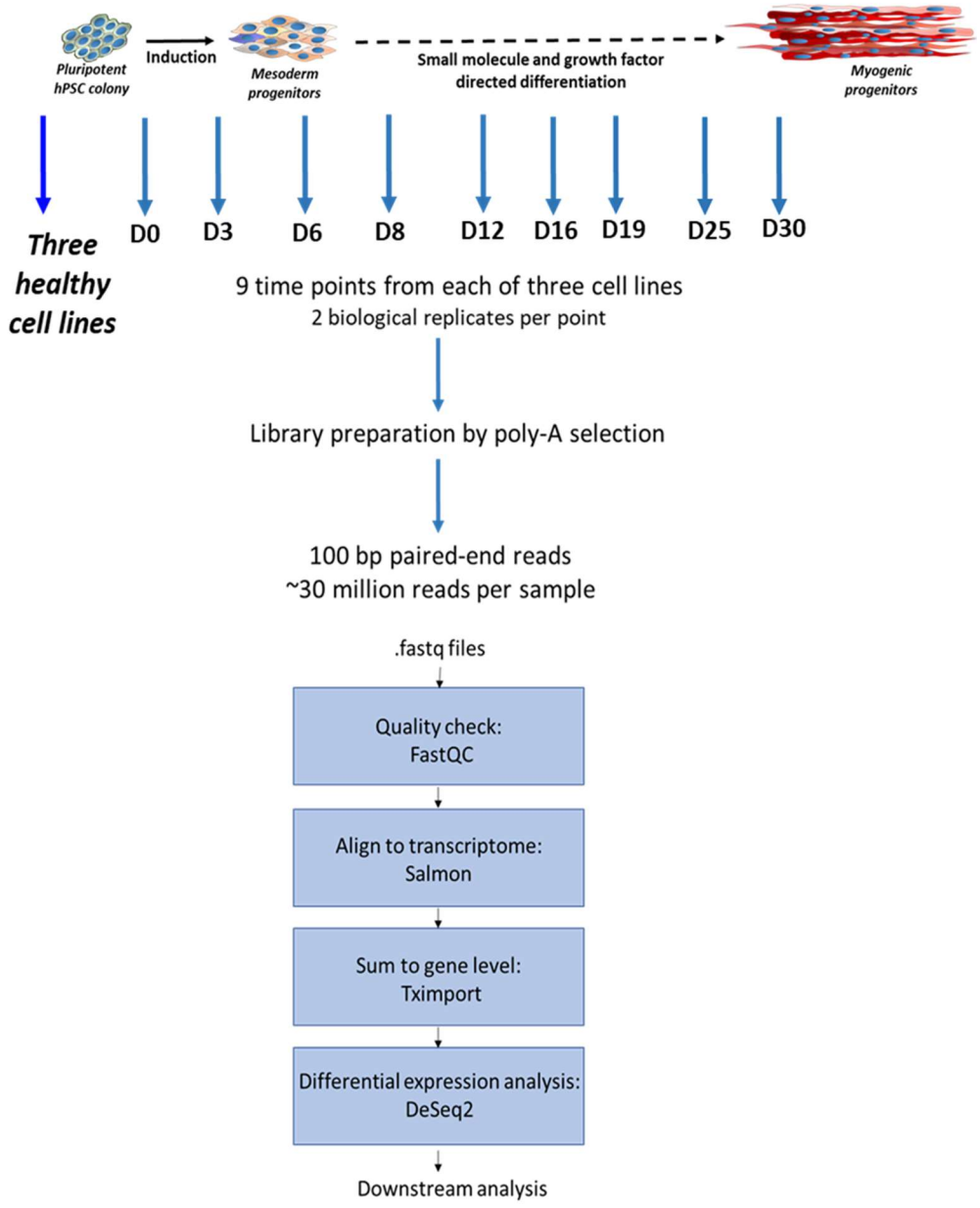

Fig. S3 Experimental schematic with downstream bioinformatics pipeline

Three hiPSC lines from healthy individual were differentiated in parallel according to a published protocol for myogenic differentiation with samples taken for RNA sequencing at nine timepoints. Pipeline for analysis is detailed above. See also Methods.

Figure S4

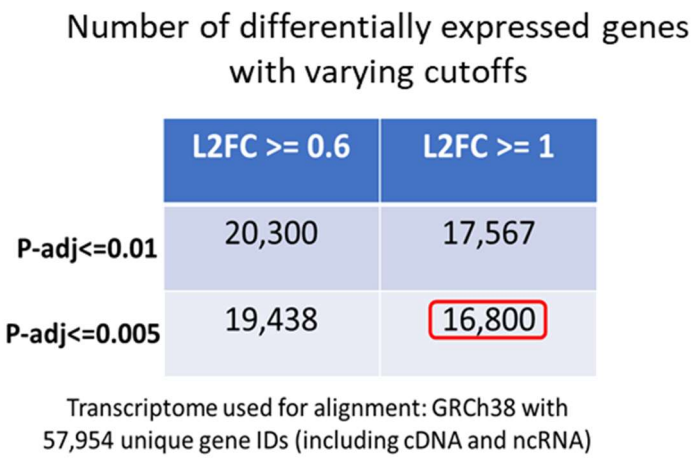

Fig. S4 Comparison of four L2FC and p-value cutoff conditions for differentially expressed genes

After differential expression (DE) analysis, we compare the number of significantly DE genes with varied L2FC and p-value cutoffs. Adjusting L2FC results in more genes that are filtered out, indicating there are a large percent of genes that have low fold change in their expression, but may still be statistically significant. Due to the large number of total DEGs (across all time points and cell lines) we set cut-offs at p-adj <-0.005 and L2FC >=1 for a total of 16,800 DEGs for downstream analysis.

Figure S5

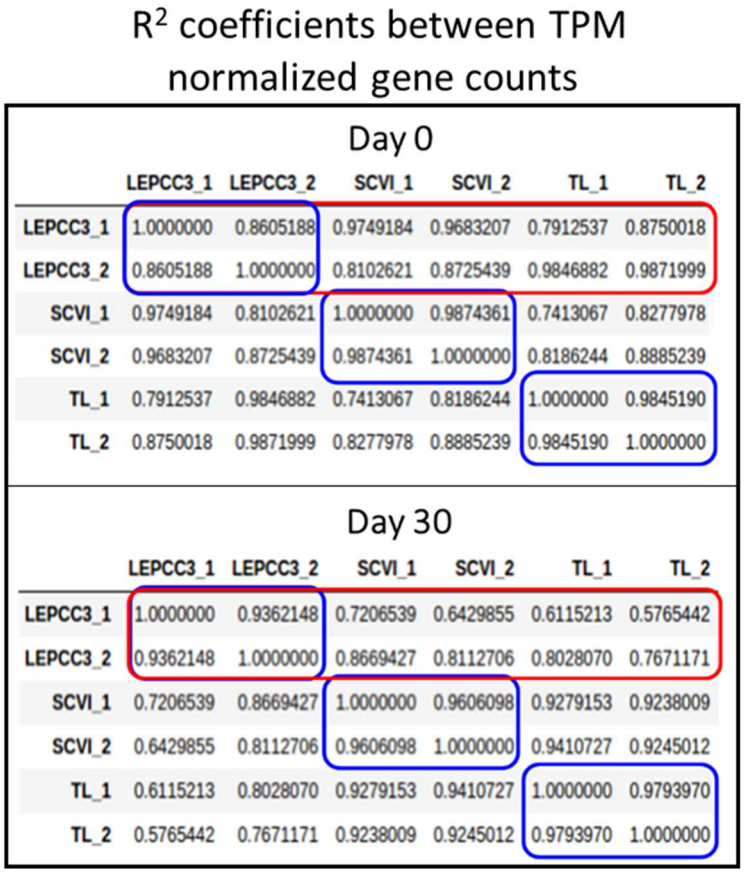

Fig. S5 TPM normalized gene count correlation is high between same-cell line replicates, and progressively lower between different lines with increased time of differentiation

Blue boxes show R^2 coefficient between TPM normalized gene counts of biological replicates from the same cell line. At day zero and day thirty of differentiation, these values remain high, indicating consistent differentiation in the same cell line. Red boxes show R^2 coefficient calculated between replicates of different cell lines. While these are relatively high on day zero of differentiation, by day thirty they are lower, indicating disparate gene expression patterns between different cell lines.

Figure S6

Differentiation-related enrichment terms	P-value
Neural Crest Differentiation_Homo sapiens_WP2064	1.202e-9
Endoderm Differentiation_Homo sapiens_WP2853	5.160e-5
Cardiac Progenitor Differentiation_Homo sapiens_WP2406	8.208e-5
Senescence and Autophagy in Cancer_Homo sapiens_WP615	5.961e-4
Endochondral Ossification_Homo sapiens_WP474	1.806e-3
Mesodermal Commitment Pathway_Homo sapiens_WP2857	3.835e-3
Dopaminergic Neurogenesis_Homo sapiens_WP2855	7.778e-3
Ectoderm Differentiation_Homo sapiens_WP2858	1.217e-2
Wnt Signaling Pathway_Homo sapiens_WP428	1.329e-2
Primary Focal Segmental Glomerulosclerosis FSGS_Homo sapiens_WP2572	1.693e-2

Pluripotency-related enrichment terms	P-value
Wnt Signaling Pathway and Pluripotency_Homo sapiens_WP399	8.069e-4
Preimplantation Embryo_Homo sapiens_WP3527	1.789e-3
SIDS Susceptibility Pathways_Homo sapiens_WP706	2.689e-3
Mesodermal Commitment Pathway_Homo sapiens_WP2857	5.389e-3
Cardiac Progenitor Differentiation_Homo sapiens_WP2406	7.793e-3
Notch Signaling Pathway_Homo sapiens_WP61	1.339e-2
Endoderm Differentiation_Homo sapiens_WP2853	2.106e-2
Cori Cycle_Homo sapiens_WP1946	2.285e-2
Vitamin A and Carotenoid Metabolism_Homo sapiens_WP716	2.562e-2
Imatinib Resistance in Chronic Myeloid Leukemia_Homo sapiens_WP2946	3.775e-2

Fig. S6 Differentiation and pluripotency associated gene modules have corresponding enrichment

In Fig 3A and 3B we identified gene modules associated with key transcriptional regulators of pluripotency and differentiation, respectively. The above biological pathway enrichment terms corroborate that the hierarchical clustering to identify the gene modules correspond to differentiation and pluripotency related processes.

Figure S7

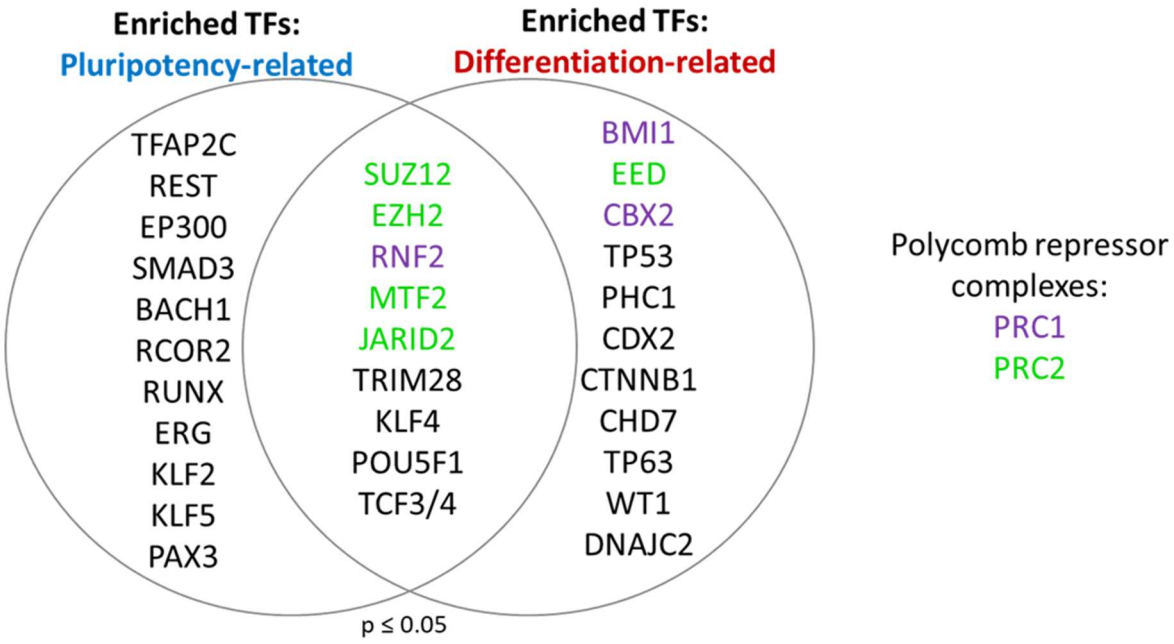

Fig. S7 Polycomb repressor complex (PRC) components are enriched transcription factors for gene modules related to pluripotency and differentiation

Enriched transcription factors were determined for pluripotency-related gene modules (Fig 3A) and differentiation-related gene modules (Fig 3B), with p<=0.05. Regulatory transcription factors common to both groups included multiple components of chromatin modification complexes PRC 1 (purple) and PRC2 (green).

Enriched TFs were determined with Enrichr (http://amp.pharm.mssm.edu/Enrichr/), using the Chea database.

Figure S8

Effector	Activity	References
CHIR (exogenous small molecule)	Wnt pathway activation by increasing the nuclear translocation of β-catenin via GSK3β inhibition. Multiple hPSC differentiation protocols to mesendoderm-derived lineages utilize CHIR for initial specification	*(13)*
LDN (exogenous small molecule)	Selective modulation of TGFβ family pathways	*(13)*
Wnt pathway	Downstream effects include increase in β-catenin mediated transcriptional activity.	*(31,32)*
Notch pathway	Signals through multiple downstream effectors, including transcription factors HES7 and LEF1	*(32,53)*
TGFβ pathway	Signals through multiple downstream effectors, including SMAD family transcription factors.	*(30)*
NuRD/TRIM28 (epigenetic)	Through TRIM28, NuRD targets several regulators of pluripotency, including POU5F1	*(27,28)*
PRC1/2 (epigenetic regulation)	Well-known epigenetic regulators of pluripotency, priming. Targets include pluripotency regulators POU5F1, NANOG, as well as β-catenin cofactors SMAD, ZIC	*(23-25)*
NANOG	Transcriptional regulator of pluripotency, with numerous targets including key transcriptional regulators of differentiation T, EOMES	*(37,40)*
POU5F1	Key transcriptional regulator of pluripotency, with numerous targets including key transcriptional regulators of differentiation T, EOMES, as well as TLE family of β-catenin cofactors.	*(54)*
T	Key regulator of mesendoderm differentiation, it is a transcriptional target of β-catenin. Also regulates and is regulated by pluripotency TFs POU5F1, NANOG	*(42)*
EOMES	Regulator of endoderm differentiation, it is a transcriptional target of β-catenin. Also regulates and is regulated by pluripotency TFs POU5F1, NANOG	*(42)*
TCF	Family of β-catenin transcriptional cofactors. Physically interact with LEF1, TLE, β-catenin	*(31,32)*
LEF1	β-catenin transcriptional cofactor. Aso mediates crosstalk between Notch and Wnt pathways. Physically interacts with LEF1, TCF, β-catenin	*(32)*
HES7	Downstream effector of Notch pathway, and interacts with β-catenin cofactors TLE	*(55)*
SMAD	Downstream effectors of TGFβ pathway. Modulates intranuclear β-catenin activity via direct physical interaction	*(29)*
ZIC	β-catenin transcriptional cofactor, as well as PRC1 targets. ZIC3 regulates Nanog expression through interaction with NANOG promoter.	*(30,40)*
TLE	β-catenin transcriptional cofactors. Physically interact with LEF1, TCF, β-catenin. With HES7, may modulate Wnt and Notch pathway crosstalk.	*(33,39,55)*
β-catenin	Downstream effector of Wnt pathway. Transcriptional activity modulated by exogenous cues, epigenetics, transcriptional and pathways to effect differentiation, including T, EOMES expression	*(33)*

Fig. S8 Interactions between components of network in Fig. 6A

This table lists the details of interactions between exogeneous cues, pathways, transcription factors, and epigenetic regulation, with β-catenin cofactors and downstream targets. The network schematic (Fig. 7A) is based on this table.

Figure S9

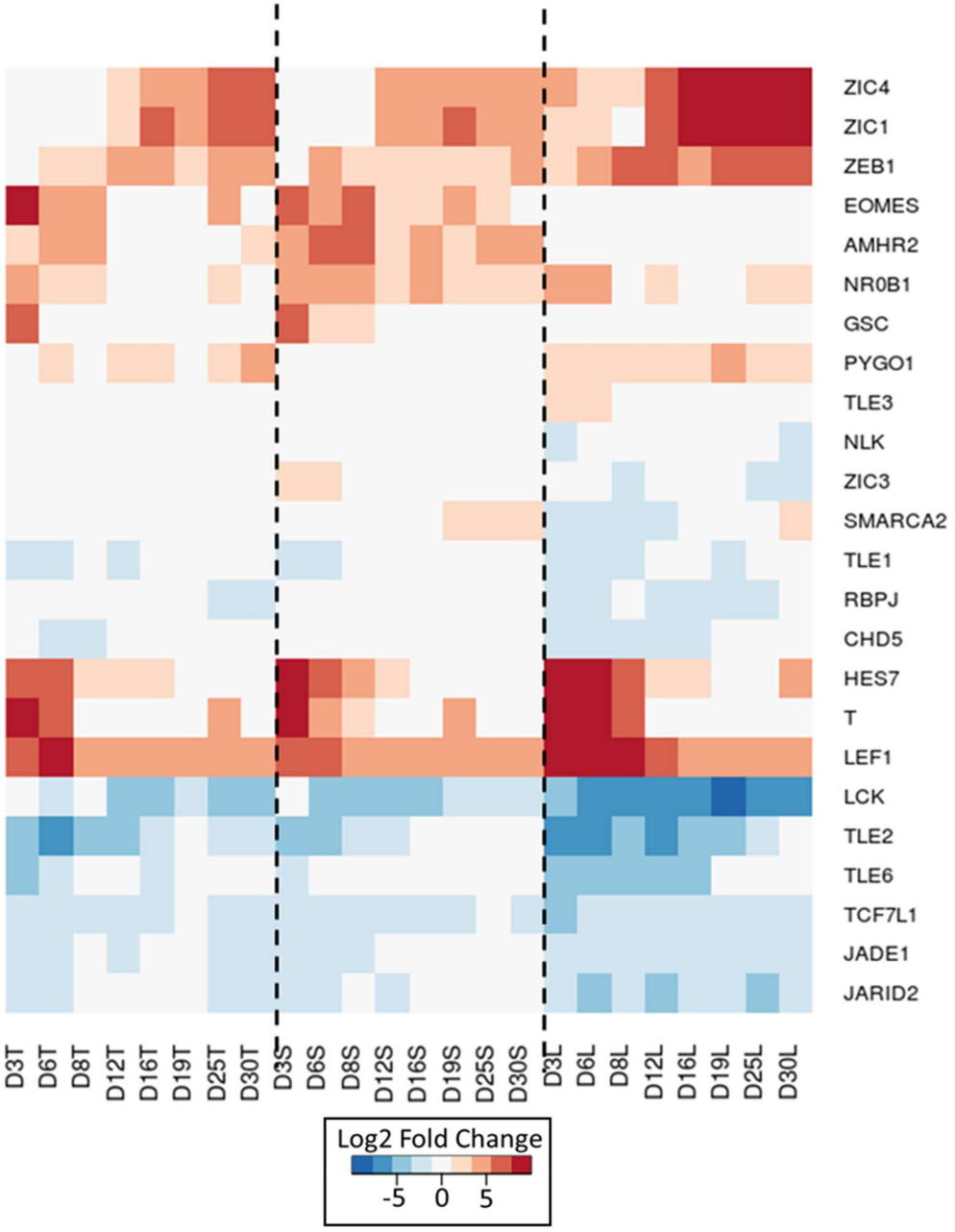

Fig. S9 Cell line-dependent expression of β-catenin transcriptional cofactors and targets

We selected transcriptional cofactors and targets of β-catenin that had cell line-dependent expression, particularly at the outset of differentiation, as targets for siRNA-mediated knockdown to test our model (Fig 5D). Genes of particular interest were those that were upregulated in the lines with blunted myogenesis, or those that were downregulated in the line with robust myogenesis at the outset of differentiation; their knockdown in lines with blunted myogenesis might then more closely resemble gene expression of the promyogenic line.

Figure S10

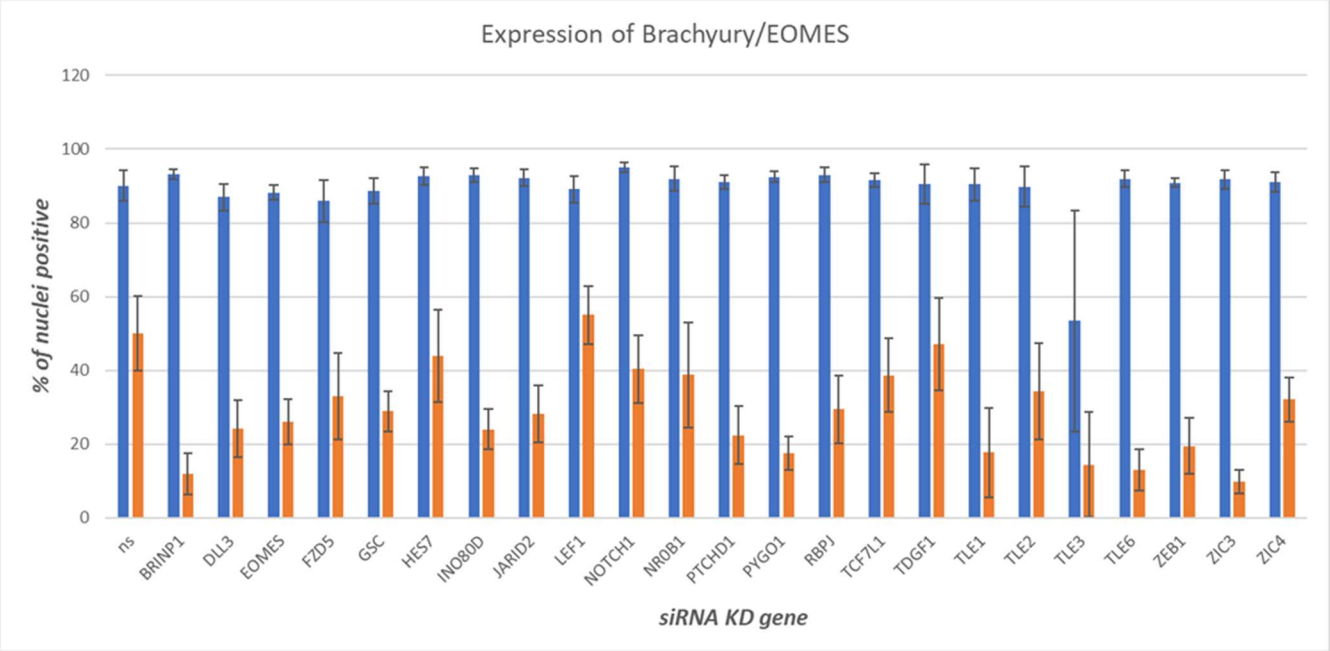

Fig. S10 Brachyury and EOMES expression at day three of differentiation after gene knockdown screen in a cell line with blunted myogenesis

Results of siRNA mediated knockdown of genes in Fig S8. Cells were transfected with siRNA at day zero and differentiated for three days before IF staining for Brachyury (blue) and Eomes (orange). Percent of nuclei positive were calculated with automated imaging and quantification (MetaXpress software). Brachyury expression is high in most experimental conditions, as expected with exogenous CHIR. About half of nuclei are positive for Eomes in the nonspecific control, as well as with LEF1 and TDGF1 knockdown. Eomes is low in ZIC3 knockdown as well as several other conditions; however, several other conditions suffered from poor cell viability for longer differentiation times on retest.

REFERENCES AND NOTES

1. S. M. Wu, K. Hochedlinger, Harnessing the potential of induced pluripotent stem cells for regenerative medicine. *Nat. Cell Biol.* **13**, 497–505 (2011).

2. N. Jiwlawat, E. Lynch, J. Jeffrey, J. M. Van Dyke, M. Suzuki, Current progress and challenges for skeletal muscle differentiation from human pluripotent stem cells using transgene-free approaches. *Stem Cells Int.* **2018**, 6241681 (2018).

3. J. Chal, O. Pourquié, Making muscle: Skeletal myogenesis in vivo and in vitro. *Development* **144**, 2104–2122 (2017).

4. A. Trounson, N. D. DeWitt, Pluripotent stem cells progressing to the clinic. *Nat. Rev. Mol. Cell Biol.* **17**, 194–200 (2016).

5. J. Bilic, J. C. I. Belmonte, Concise review: Induced pluripotent stem cells versus embryonic stem cells: Close enough or yet too far apart? *Stem Cells* **30**, 33–41 (2012).

6. H. M. Blau, G. K. Pavlath, E. C. Hardeman, C. P. Chiu, L. Silberstein, S. G. Webster, S. C. Miller, C. Webster, Plasticity of the differentiated state. *Science* **230**, 758–766 (1985).

7. Y. Hwang, A. Phadke, S. Varghese, Engineered microenvironments for self-renewal and musculoskeletal differentiation of stem cells. *Regen. Med.* **6**, 505–524 (2011).

8. K. Mukund, S. Subramaniam, Skeletal muscle: A review of molecular structure and function, in health and disease. *WIREs Syst. Biol. Med.* **12**, e1462 (2020).

9. C. S. Young, M. R. Hicks, N. V. Ermolova, H. Nakano, M. Jan, S. Younesi, S. Karumbayaram, C. Kumagai-Cresse, D. Wang, J. A. Zack, D. B. Kohn, A. Nakano, S. F. Nelson, M. C. Miceli, M. J. Spencer, A. D. Pyle, A single CRISPR-Cas9 deletion strategy that targets the majority of DMD patients restores dystrophin function in hiPSC-derived muscle cells. *Cell Stem Cell* **18**, 533–540 (2016).

10. Y. Hwang, S. Suk, S. Lin, M. Tierney, B. Du, T. Seo, A. Mitchell, A. Sacco, S. Varghese, Directed in vitro myogenesis of human embryonic stem cells and their in vivo engraftment. *PLOS ONE* **8**, e72023 (2013).

11. J. Chal, M. Oginuma, Z. Al Tanoury, B. Gobert, O. Sumara, A. Hick, F. Bousson, Y. Zidouni, C. Mursch, P. Moncuquet, O. Tassy, S. Vincent, A. Miyanari, A. Bera, J.-M. Garnier, G. Guevara, M. Hestin, L. Kennedy, S. Hayashi, B. Drayton, T. Cherrier, B. Gayraud-Morel, E. Gussoni, F. Relaix, S. Tajbakhsh, O. Pourquié, Differentiation of pluripotent stem cells to muscle fiber to model Duchenne muscular dystrophy. *Nat. Biotechnol.* **33**, 962–969 (2015).

12. H. Xi, W. Fujiwara, K. Gonzalez, M. Jan, S. Liebscher, B. V. Handel, K. Schenke-Layland, A. D. Pyle, In vivo human somitogenesis guides somite development from hPSCs. *Cell Rep.* **18**, 1573–1585 (2017).

13. J. Chal, Z. Al Tanoury, M. Hestin, B. Gobert, S. Aivio, A. Hick, T. Cherrier, A. P. Nesmith, K. K. Parker, O. Pourquié, Generation of human muscle fibers and satellite-like cells from human pluripotent stem cells in vitro. *Nat. Protoc.* **11**, 1833–1850 (2016).

14. M. J. Boland, K. L. Nazor, J. F. Loring, Epigenetic regulation of pluripotency and differentiation. *Circ. Res.* **115**, 311–324 (2014).

15. G. Guo, F. von Meyenn, M. Rostovskaya, J. Clarke, S. Dietmann, D. Baker, A. Sahakyan, S. Myers, P. Bertone, W. Reik, K. Plath, A. Smith, Epigenetic resetting of human pluripotency. *Development* **144**, 2748–2763 (2017).

16. G. Liang, Y. Zhang, Genetic and epigenetic variations in iPSCs: Potential causes and implications for application. *Cell Stem Cell* **13**, 149–159 (2013).

17. P. Langfelder, B. Zhang, S. Horvath, Defining clusters from a hierarchical cluster tree: The Dynamic Tree Cut package for R. *Bioinformatics* **24**, 719–720 (2008).

18. A. Fico, A. Fiorenzano, E. Pascale, E. J. Patriarca, G. Minchiotti, Long non-coding RNA in stem cell pluripotency and lineage commitment: Functions and evolutionary conservation. *Cell. Mol. Life Sci.* **76**, 1459–1471 (2019).

19. M. Keshavarz, M. H. Asadi, Long non-coding RNA ES1 controls the proliferation of breast cancer cells by regulating the Oct4/Sox2/miR-302 axis. *FEBS J.* **286**, 2611–2623 (2019).

20. K. M. Pineault, D. M. Wellik, Hox genes and limb musculoskeletal development. *Curr. Osteoporos. Rep.* **12**, 420–427 (2014).

21. B. De Kumar, R. Krumlauf, HOXs and lincRNAs: Two sides of the same coin. *Sci. Adv.* **2**, e1501402 (2016).

22. E. Y. Chen, C. M. Tan, Y. Kou, Q. Duan, Z. Wang, G. V. Meirelles, N. R. Clark, A. Ma'ayan, Enrichr: Interactive and collaborative HTML5 gene list enrichment analysis tool. *BMC Bioinformatics* **14**, 128 (2013).

23. L. Aloia, B. Di Stefano, L. Di Croce, Polycomb complexes in stem cells and embryonic development. *Development* **140**, 2525–2534 (2013).

24. R. S. Illingworth, J. J. Hölzenspies, F. V. Roske, W. A. Bickmore, J. M. Brickman, Polycomb enables primitive endoderm lineage priming in embryonic stem cells. *eLife* **5**, e14926 (2016).

25. Z. Zhang, A. Jones, C.-W. Sun, C. Li, C.-W. Chang, H.-Y. Joo, Q. Dai, M. R. Mysliwiec, L.-C. Wu, Y. Guo, W. Yang, K. Liu, K. M. Pawlik, H. Erdjument-Bromage, P. Tempst, Y. Lee, J. Min, T. M. Townes, H. Wang, PRC2 complexes with JARID2, MTF2, and esPRC2p48 in ES cells to modulate ES cell pluripotency and somatic cell reprograming. *Stem Cells* **29**, 229–240 (2011).

26. P. J. Ho, S. M. Lloyd, X. Bao, Unwinding chromatin at the right places: How BAF is targeted to specific genomic locations during development. *Development* **146**, dev178780 (2019).

27. S. K. Hota, B. G. Bruneau, ATP-dependent chromatin remodeling during mammalian development. *Development* **143**, 2882–2897 (2016).

28. U. Oleksiewicz, M. Gładych, A. T. Raman, H. Heyn, E. Mereu, P. Chlebanowska, A. Andrzejewska, B. Sozańska, N. Samant, K. Fąk, P. Auguścik, M. Kosiński, J. P. Wróblewska, K. Tomczak, K. Kulcenty, R. Płoski, P. Biecek, M. Esteller, P. K. Shah, K. Rai, M. Wiznerowicz, TRIM28 and

Interacting KRAB-ZNFs control self-renewal of human pluripotent stem cells through epigenetic repression of Pro-differentiation genes. *Stem Cell Rep.* **9**, 2065–2080 (2017).

29. B. Braschi, P. Denny, K. Gray, T. Jones, R. Seal, S. Tweedie, B. Yates, E. Bruford, Genenames.org: The HGNC and VGNC resources in 2019. *Nucleic Acids Res.* **47**, D786–D792 (2019).

30. H. Kempf, R. Olmer, A. Haase, A. Franke, E. Bolesani, K. Schwanke, D. Robles-Diaz, M. Coffee, G. Göhring, G. Dräger, O. Pötz, T. Joos, E. Martinez-Hackert, A. Haverich, F. F. R. Buettner, U. Martin, R. Zweigerdt, Bulk cell density and Wnt/TGFbeta signalling regulate mesendodermal patterning of human pluripotent stem cells. *Nat. Commun.* **7**, 13602 (2016).

31. C. C. Anthony, D. J. Robbins, Y. Ahmed, E. Lee, Nuclear regulation of Wnt/β-catenin signaling: It's a complex situation. *Genes* **11**, 11080886 (2020).

32. J. Galceran, C. Sustmann, S.-C. Hsu, S. Folberth, R. Grosschedl, LEF1-mediated regulation of Delta-like1 links Wnt and Notch signaling in somitogenesis. *Genes Dev.* **18**, 2718–2723 (2004).

33. F.-I. Lu, Y.-H. Sun, C.-Y. Wei, C. Thisse, B. Thisse, Tissue-specific derepression of TCF/LEF controls the activity of the Wnt/β-catenin pathway. *Nat. Commun.* **5**, 5368 (2014).

34. J. Ernst, Z. Bar-Joseph, STEM: A tool for the analysis of short time series gene expression data. *BMC Bioinformatics* **7**, 191 (2006).

35. J. Zhang, E. Nuebel, G. Q. Daley, C. M. Koehler, M. A. Teitell, Metabolic regulation in pluripotent stem cells during reprogramming and self-renewal. *Cell Stem Cell* **11**, 589–595 (2012).

36. W. Fu, P. Asp, B. Canter, B. D. Dynlacht, Primary cilia control hedgehog signaling during muscle differentiation and are deregulated in rhabdomyosarcoma. *Proc. Natl. Acad. Sci. U.S.A.* **111**, 9151–9156 (2014).

37. S. Mendjan, V. L. Mascetti, D. Ortmann, M. Ortiz, D. W. Karjosukarso, Y. Ng, T. Moreau, R. A. Pedersen, NANOG and CDX2 pattern distinct subtypes of human mesoderm during exit from pluripotency. *Cell Stem Cell* **15**, 310–325 (2014).

38. S. Tripathi, T. Miyake, J. C. McDermott, Smad7:β-catenin complex regulates myogenic gene transcription. *Cell Death Dis.* **10**, 387–399 (2019).

39. Z. Zhao, L. Wang, E. Bartom, S. Marshall, E. Rendleman, C. Ryan, A. Shilati, J. Savas, N. Chandel, A. Shilatifard, β-Catenin/Tcf7l2–dependent transcriptional regulation of GLUT1 gene expression by Zic family proteins in colon cancer. *Sci. Adv.* **5**, eaax0698 (2019).

40. L. S. Lim, F. H. Hong, G. Kunarso, L. W. Stanton, The pluripotency regulator Zic3 is a direct activator of the Nanog promoter in ESCs. *Stem Cells* **28**, 1961–1969 (2010).

41. D. Szklarczyk, A. L. Gable, D. Lyon, A. Junge, S. Wyder, J. Huerta-Cepas, M. Simonovic, N. T. Doncheva, J. H. Morris, P. Bork, L. J. Jensen, C. von Mering, STRING v11: Protein–protein association networks with increased coverage, supporting functional discovery in genome-wide experimental datasets. *Nucleic Acids Res.* **47**, D607–D613 (2019).

42. J. Tosic, G.-J. Kim, M. Pavlovic, C. M. Schröder, S.-L. Mersiowsky, M. Barg, A. Hofherr, S. Probst, M. Köttgen, L. Hein, S. J. Arnold, Eomes and Brachyury control pluripotency exit and germ-layer segregation by changing the chromatin state. *Nat. Cell Biol.* **21**, 1518–1531 (2019).

43. T. J. Fujimi, M. Hatayama, J. Aruga, Xenopus Zic3 controls notochord and organizer development through suppression of the Wnt/β-catenin signaling pathway. *Dev. Biol.* **361**, 220–231 (2012).

44. G. C. Schoenwolf, S. B. Bleyl, P. R. Brauer, P. H. Francis-West, *Larsen's Human Embryology* (Churchill Livingstone/Elsevier, ed. 5, 2009).

45. C. Alev, Y. Wu, T. Kasukawa, L. M. Jakt, H. R. Ueda, G. Sheng, Transcriptomic landscape of the primitive streak. *Development* **137**, 2863–2874 (2010).

46. A. S. T. Smith, S. L. Passey, N. R. W. Martin, D. J. Player, V. Mudera, L. Greensmith, M. P. Lewis, Creating interactions between tissue-engineered skeletal muscle and the peripheral nervous system. *Cells Tissues Organs* **202**, 143–158 (2016).

47. P. Ewels, M. Magnusson, S. Lundin, M. Käller, MultiQC: Summarize analysis results for multiple tools and samples in a single report. *Bioinformatics* **32**, 3047–3048 (2016).

48. R. Patro, G. Duggal, M. I. Love, R. A. Irizarry, C. Kingsford, Salmon: Fast and bias-aware quantification of transcript expression using dual-phase inference. *Nat. Methods* **14**, 417–419 (2017).

49. C. Soneson, M. I. Love, M. D. Robinson, Differential analyses for RNA-seq: Transcript-level estimates improve gene-level inferences. *F1000Res.* **4**, 1521–1540 (2015).

50. M. I. Love, W. Huber, S. Anders, Moderated estimation of fold change and dispersion for RNA-seq data with DESeq2. *Genome Biol.* **15**, 550–571 (2014).

51. R Core Team, *R: A Language and Environment for Statistical Computing* (R Foundation for Statistical Computing, 2014); http://www.R-project.org/.

52. M. V. Kuleshov, M. R. Jones, A. D. Rouillard, N. F. Fernandez, Q. Duan, Z. Wang, S. Koplev, S. L. Jenkins, K. M. Jagodnik, A. Lachmann, M. G. McDermott, C. D. Monteiro, G. W. Gundersen, A. Ma'ayan, Enrichr: A comprehensive gene set enrichment analysis web server 2016 update. *Nucleic Acids Res.* **44**, W90–W97 (2016).

53. A. F. Laing, S. Lowell, J. M. Brickman, Gro/TLE enables embryonic stem cell differentiation by repressing pluripotent gene expression. *Dev. Biol.* **397**, 56–66 (2015).

54. C. Mulas, G. Chia, K. A. Jones, A. C. Hodgson, G. G. Stirparo, J. Nichols, Oct4 regulates the embryonic axis and coordinates exit from pluripotency and germ layer specification in the mouse embryo. *Development* **145**, dev159103 (2018).

55. M. Buscarlet, S. Stifani, The 'Marx' of Groucho on development and disease. *Trends Cell Biol.* **17**, 353–361 (2007).